

# Multi-Modal Brain-Computer Interface (BCI) Glasses: Integrating Few-Channel fNIRS, EEG, and EOG to Robustly and Practically Monitor Cognitive Load

*Karim Ed Al, Yale University, Yale, New Haven, CT, 06520, United States*

*Minsol Kim, Wellesley College, Wellesley, MA, 02481, United States*

*Nataliya Kosmyna, MIT Media Lab, Cambridge, MA, 02139, United States*

## Abstract

This work presents a few-channel brain-computer interface (BCI) device that integrates multiple sensing modalities into a glasses form-factor practical for everyday use. In the last decade a rapidly growing number of BCI studies have utilized multiple brain-sensing modalities to exploit their complementary information content and differing error sources. They demonstrated, using research-grade devices with dozens of data channels, that a multimodal approach can improve the accuracy, robustness, information transfer rate, and ease of use of BCI systems. These factors remain a challenge for non-invasive BCIs, especially the compact consumer-grade devices that have been developed and commercialized in recent years. The goal of this project was to help alleviate these issues which have limited the usefulness and prevented the widespread adoption of consumer BCIs. To the best of our knowledge, we have developed a prototype of the first BCI device to integrate both electrophysiological sensing and hemodynamic sensing into a compact wearable device suitable for consumers. More specifically, our BCI glasses fuse two electroencephalography (EEG) channels, four functional near-infrared spectroscopy (fNIRS) channels, and one electrooculography (EOG) channel while retaining a comfortable and socially acceptable design. In this study, we validated this platform by having 14 subjects perform a cognitive load task consisting of mental arithmetic with visual, auditory, and imagined stimuli. Offline classification using an SVM produced an increased average accuracy of 76.3% compared with 69.6% and 65.4% for EEG and fNIRS respectively. We conclude that the integration of few-channel fNIRS and EEG into practical form factors could help overcome several of the challenges holding back the adoption of consumer BCIs.

## 1. Introduction

BCIs measure the user's brain activity and translate it into control signals that are sent to an external device. BCIs recognize patterns in the user's brain activity, which are associated with different mental states or processes, to establish a novel communication channel between the user's brain and digital devices. BCIs do not rely on the normal neuromuscular output pathways from the brain which are limited in bandwidth and information content and can be disrupted by spinal cord injuries or neurodegenerative diseases.

Although some BCIs utilize surgically implanted sensors, the risks associated with such procedures prevent their widespread adoption in the near term. Most research has thus focused on non-invasive BCIs that utilize extracranial sensors to monitor brain activity. Non-invasive BCIs have demonstrated exciting capabilities including allowing paralyzed individuals to control robotic arms or wheelchairs, enabling completely locked-in ALS patients to communicate with

others, and helping to rehabilitate stroke victims [Meng et al., 2016; ]. In addition to numerous other medical applications, BCIs have been demonstrated to have many use cases for healthy individuals in personal and professional settings. These consumer applications include *Brain fingerprinting for lie detection* (Farwell et al., 2014), *detecting drowsiness for improving human working performances* (Aricò et al., 2016; Wei et al., 2018), *estimating reaction time* (Wu et al., 2017b), *controlling virtual reality* (Vourvopoulos et al., 2019), *quadcopters* (LaFleur et al., 2013) and *video games* (Singh et al., 2020), and *driving humanoid robots* (Choi and Jo, 2013; Spataro et al., 2017)

**Current Challenges & Sensing Technology:** Despite the immense potential demonstrated by BCIs through 50 years of research, until now very few individuals have received any benefits from BCIs outside of the lab. This is mainly due to the challenge of reliably acquiring useful brain data with a device that is accessible and practical. The majority of BCI research has been conducted using expensive, complicated, bulky, non-portable, or uncomfortable devices. However, in the last two decades, advances in computing, machine learning, neuroscience, and biosensors have allowed the development of portable BCI wearables based on EEG and more recently fNIRS. Each modality only captures limited information associated with cognitive activity and has unique strengths and weaknesses which make it better suited for some tasks than others.

**EEG:** EEG was invented in the 1920s and utilizes electrodes placed on the scalp to detect postsynaptic potentials produced by neuronal firing []. All of the aforementioned BCI studies utilized EEG and it is by far the most commonly used sensing modality for BCIs due to its high temporal resolution (~50 ms), relatively low cost, and safety [Saha et al. 2021]. However, the amplitude of postsynaptic potentials is on the order of millivolts and must cross several layers of tissue to reach the EEG electrodes which further dampens the signal. Thus, EEG is only able to detect the synchronized firing of large populations of neurons in the outer layers of the cortex and has a relatively poor spatial resolution of ~1 cm. Clinical and research-grade EEGs require the application of a conducting gel that is messy, uncomfortable, and entirely impractical for everyday applications to reduce the high impedance that exists between the electrodes and scalp. For clinical and research applications, wired EEG electrodes are typically attached to the scalp using adhesive (*Figure 1a*) as electrode slippage causes significant artifacts. This requires a trained technician and significant setup time so BCI studies often use EEG caps (*Figure 1b*) which are still impractical for everyday use as they are uncomfortable and usually wired to an amplifier. Finally, EEG is highly sensitive to electrophysiological noise so to better remove artifacts these systems typically use electromyography (EMG), electrocardiography (ECG), and electrooculography (EOG) electrodes to detect electrical signals produced by muscle movements, heart beats, and eye movements or blinking respectively. These issues make purely EEG-based BCIs impractical and unreliable in everyday environments which limits their real-world applications especially for safety critical use cases.

**Consumer EEGs:** Despite these challenges several companies have developed and even commercialized consumer-grade EEG devices such as those shown in *Figure 1c*. These devices typically use dry electrodes, wireless data transmission, and rely on advanced signal processing methods to increase the signal-to-noise ratio. One of the first such devices was the NeuroSky MindWave which only has one forehead EEG electrode and one reference electrode that is clipped onto the earlobe. The Emotiv EPOC is another EEG wearable that was designed to be used by developers as a video game controller but has also been commonly used for BCI research. It utilizes 14 electrodes and two reference electrodes. Maskeliunas et al. [2016] evaluated the Emotiv EPOC and the Neurosky MindWave for control tasks using concentration/relaxation and blinking recognition tasks. This 10 person study achieved average classification accuracies of 60.5% and 22.2% for concentration/relaxation and 75.6% and 49.6% for blinking recognition by the Emotiv EPOC and NeuroSky MindWave devices respectively. The statistical analysis showed that there was high variability between subjects and that up to 50% of subjects were not able to achieve satisfactory control accuracy. This phenomenon, called BCI illiteracy, is especially acute with consumer grade devices as the low number of sensors, lower sensor quality, and less precise sensor placement hinders effective feedback between the user and the system. The authors agreed with other similar studies that consumer-grade EEG devices are currently not suitable for serious control applications and suggested that they be combined with other sensing modalities. Several of the studies have also noted that the headset device designs become uncomfortable after extended use, are prone to artifacts caused by sensor slippage, and draw attention from onlookers which can be uncomfortable and distracting [Maskeliunas et al., 2016; Vourvopoulos & Liarokapis, 2014]. Newer devices such as the Idun Guardian earbuds, Neurable Enten headphones, and AttentivU glasses (described in section 2.1.1) thus have much more socially-acceptable form factors.



(a)



(b)

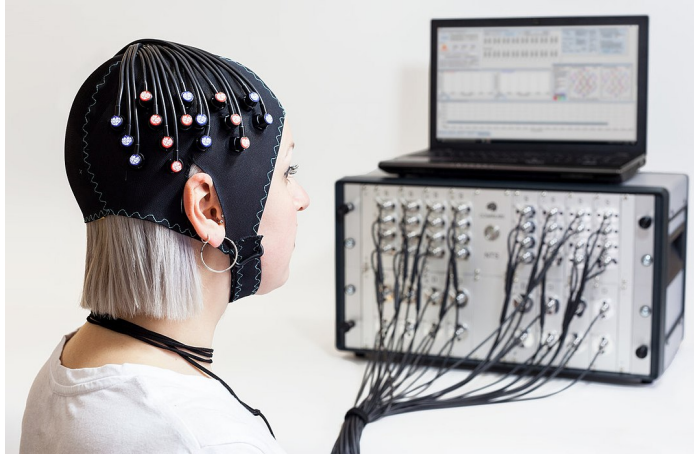


**Figure 1:** (a) Standard EEG with electrodes glued to scalp and wired to an amplifier (b) EEG cap with EOG/EMG electrodes on face and ECG electrodes on chest for artifact removal (b) Consumer-grade EEG-based wearable BCIs

**fNIRS:** fNIRS is an optical neuroimaging modality that was first adapted for BCIs in 2004 by Coyle et al. and has since become the most commonly used BCI modality aside from EEG [Kwon et al., 2020]. Like fMRI, fNIRS exploits the fact that increased neuronal firing is locally correlated with increased blood flow and oxygen consumption. Each fNIRS channel, known as an optode, consists of an emitter and a detector which are placed on the scalp. The emitter produces at least two wavelengths of near-infrared (NIR) light (600-1000 nm) which diffuses through the underlying tissue while the detector measures the amount of NIR light reflected back out of the head. The skin and scalp are relatively transparent to NIR light while oxygenated (HbO) and deoxygenated (HbR) hemoglobin in the blood absorb different proportions of NIR light at different wavelengths. The Modified Beer-Lambert Law (described in Section 2.4.2) can then be used to calculate changes in HbO and HbR concentration which indicate changes in the amount of local neuronal firing [Delpy et al]. Like EEG, fNIRS is relatively affordable, portable, and completely safe.

fNIRS better for astronaut, racing drivers, fighter pilots for focus training as it is less susceptible to motion artifacts

**Consumer fNIRS:** While there are several wearable fNIRS devices such as the OBELAB NIRSIT intended for clinical or research applications, only one is oriented towards consumers. The Mendi headband is a consumer neurofeedback device that uses data from 3 fNIRS channels as inputs to a game designed to train focus. The relative lack of commercially available fNIRS-based BCIs is largely due to the fact that this technology is much newer than EEG. However, several other consumer-grade devices including the Blueberry (described in *Section 2.1.2*) are currently in development and available for pre-order.



(a)

<b>Mendi</b>  \$499 3 channels	<b>Blueberry</b>  \$995 2 channels	<b>NIRSiT</b>  \$? 48 channels
--	--	--

(b)

**Figure 2:** (a) Typical fNIRS setup used for clinical and research applications (b) Wearable fNIRS-based BCIs

**Multimodal BCIs:** Multimodal BCIs utilize multiple sensing modalities of which some may detect physiological signals but at least one must measure neurological activity. Most multimodal BCIs fuse simultaneous data streams from complementary sensing modalities to compensate for each other's weaknesses and more comprehensively characterize brain activity.

Research on multimodal BCIs has increased exponentially in the last decade as numerous studies have demonstrated that they are able to achieve greater classification accuracy, robustness to noise, and information transfer rate compared with unimodal BCIs [Fazli et al., 2012; Shin et al., 2017; Khan et al., 2014; Khan et al., 2017]. Multimodal BCIs are most commonly based on EEG and EOG or EEG and fNIRS [Hong & Khan, 2017]. EOG is typically used to remove motion artifacts in EEG data that are caused by eye movements and blinks. When EEG and fNIRS are used together, their features are typically combined to improve classification accuracy. EEG and fNIRS are highly complementary as resulting BCIs retain the fast signal detection time of EEG and the robustness to noise of fNIRS .

The main challenge of multimodal BCIs is their increased physical and computational complexity. Therefore, affordable and portable multimodal BCIs were not feasible previous to recent advances in machine learning, computing, and biosensing. Despite the large number of studies that have demonstrated the benefits of EEG-fNIRS BCIs, to the best of our knowledge, only two of these have investigated few-channel systems [Ahn & Jun, 2017]. Ge et al. [] achieved 81.2% average classification accuracy in a motor imagery task using three EEG channels and 10 fNIRS channels (six emitters, six detectors). This bimodal system outperformed its unimodal EEG and fNIRS components, with 6.5% and 24.4% higher accuracy, respectively. However, in this study fNIRS was recorded from central areas over the primary motor cortex where extensive preparatory work is required for many people to prevent dark, thick hairs from

blocking the NIR light. Furthermore, optimal channels were selected from an impractical EEG-fNIRS cap. Kwon et al. [2020] classified three mental states (mental arithmetic, motor imagery, and idle state) with an accuracy of  $77.6 \pm 12.1\%$  using two EEG channels and two fNIRS channels. However, once again, they selected the optimal channels from 11 EEG electrodes and thirty-six potential fNIRS optodes. Both of these studies concluded that a compact integrated fNIRS-EEG BCI would be feasible and beneficial. However, to the best of our knowledge no such wearables have been developed commercial BCI devices utilize more than one brain sensing modality an

We chose to integrate these modalities into a few-channel practical BCI system with a glasses form-factor due to their low cost, portability, safety, complementary characteristics, and the significant amount of promising previous research.

*exploiting their individual strengths; EEG provides favorable temporal resolution while fNIRS offers better spatial resolution and is robust to noise [23,24]. Additionally, EEG and fNIRS signals are associated with the neuronal electrical activity and metabolic response, respectively, providing a built-in validation for identified activity.*

While some commercially available devices combine brain sensing modalities with other physiological sensing modalities (e.g. ECG, EOG, EMG, PPG), currently none integrate multiple brain sensing modalities. (CHECK)

Although some portable multimodal BCI prototypes, such as the EEG-fNIRS cap device presented by Shin et al. [2017], have been built for research studies they are still far from practical for consumers. (results motivate our study...)

fNIRS complements EEG very well as it has relatively low temporal resolution (~1 s) but relatively high spatial resolution (~5 mm). It is similarly inexpensive, portable, and provides a new type of information that has been applied to many tasks. Furthermore, since fNIRS utilizes light it does not interfere with EEG and is not susceptible to electrical noise. However, optical changes in extracerebral layers of the head which are caused by blood pressure waves, Mayer waves, respiration, and cardiac cycles add significant noise to the signal. The light path between an emitter and detector is roughly elliptical and reaches a depth of about half of their separation distance. Many fNIRS devices use multi-distance optodes which include detectors placed relatively close to the emitter (~1 cm) that only measure these extracerebral signals. This noise can then be removed from long channels which penetrate 1-3 centimeters into the brain to isolate HbO/HbR concentration changes in the cortex [Saager et al. 2011]. Another limitation of fNIRS is that it takes several seconds for increased neuronal activation to trigger an increase in cerebral blood flow (CBF) to that area. Fazli et al. [2012] reported peak classification accuracy seven seconds after stimulus onset. However, more recent work has been able to detect a nearly instantaneous dip in HbO that precedes the increase in CBF [Hong and Zafar 2018]. Furthermore, thick dark hair blocks NIR light which decreases the signal to noise ratio and sensing depth. Thus, many fNIRS systems are placed in areas with no hair such as the forehead which is unacceptable for a user friendly device. However, alternative device designs have been proposed to solve this problem [Khan et al. 2012].

The compatibility of neurofeedback with fNIRS was demonstrated in 2012 when a coupled neurofeedback system enhanced hemodynamic changes in the brain, enabling fNIRS to better interpret motor imagery-induced activations. Kober et al. explored neurofeedback to train patients to exercise more focused control over brain activation to enhance specificity of motor imagery-induced cortical activation. Neurofeedback systems have since improved the suitability of real-time fNIRS for BCI and are now common in fNIRS studies.

## 2. Materials and Methods

### 2.1. Device

To construct our EEG-fNIRS glasses prototype and validate our hypothesis we combined two proven sensing platforms, the AttentivU EEG/EOG glasses (*Figure 3*) and Blueberry fNIRS sensors (*Figure 4*).

#### 2.1.1. AttentivU EEG/EOG Glasses

The AttentivU glasses are able to measure various cognitive processes including cognitive load, fatigue, engagement, and focus using 2 EEG channels and 1 EOG channel. AttentivU was designed to be suitable for extended use in everyday environments and to have a socially acceptable form factor. AttentivU's frame is 3D-printed from flexible nylon plastic and measures electrophysiological signals using dry electrodes made from sterling silver. Two EEG electrodes are integrated into the temple tips of the glasses and record from locations TP9 and TP10 according to the 10-20 system. One reference electrode is integrated into the nose bridge while the two EOG electrodes act as nose pads. Although not used in this experiment, the AttentivU glasses are also able to deliver auditory and vibro-tactile feedback which allow them to act as a passive biofeedback device [Kosmyna et al. 2019]. AttentivU has demonstrated performance comparable to research-grade EEGs across hundreds of subjects for target speaker detection, decoding visual imagery, and monitoring and improving engagement while driving, studying, or working [Kosmyna et al., 2022, 2019].

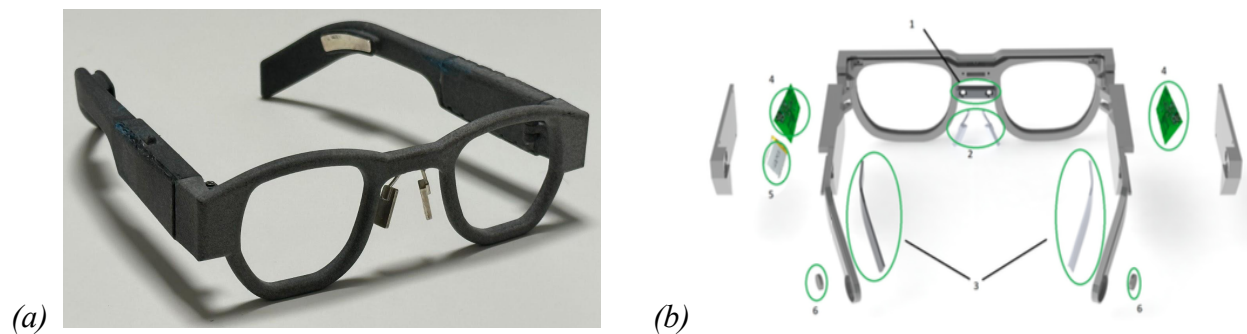


**Figure 3:** (a) The AttentivU EEG/EOG glasses. (b) Exploded view showing EOG electrodes (1), EEG reference electrode (2), EEG electrodes (3), PCBs (4), LiPo battery (5), and piezoelectric transducers to deliver auditory feedback via bone conduction (6). [Kosmyna et al., 2019]

#### 2.1.2. Blueberry fNIRS Sensor

The Blueberry is a compact Bluetooth-enabled continuous wave fNIRS sensor designed to be used by consumers in everyday contexts. One emitter produces three wavelengths of

near-infrared light (740, 840, and 950 nm) which has been shown to improve fNIRS accuracy compared to just two wavelengths [Arifler et al. 2015]. The back-scattered light is measured by two detectors located 10 mm and 27 mm away from the emitter. The penetration depth of the light that reaches each detector is roughly half of its distance from the emitter [Patil et al., 2011]. Thus, the shorter channel only measures optical changes in superficial layers of the head resulting from blood pressure waves, Mayer waves, respiration, and cardiac cycles. These extracerebral signals are present along with cerebral signals in the long channel [Saager et al. 2011]. The Blueberry's dual detector design allows us to remove this noise from the longer channel to isolate HbO/HbR concentration changes in the cortex.

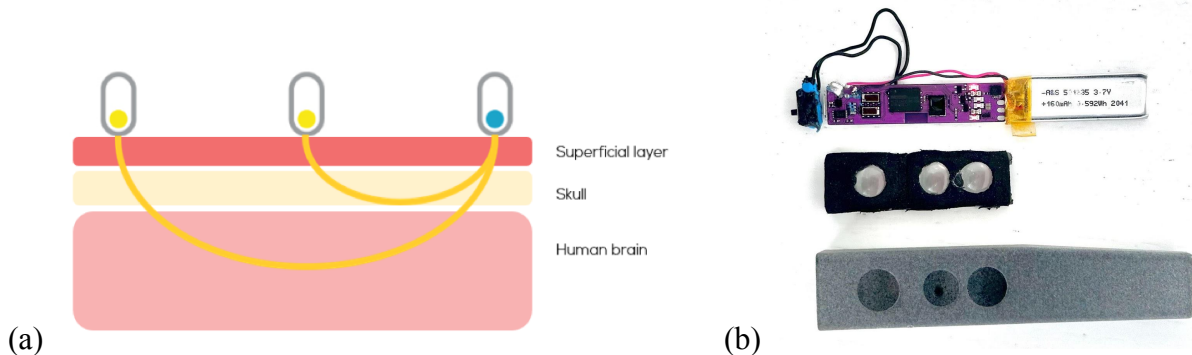


**Figure 4:** (a) fNIRS optode diagram showing emitter (blue dot), short and long separation detectors (yellow dot), and average light paths (yellow lines) through tissue. (b) Deconstructed Blueberry fNIRS sensor module showing PCB and battery (top), cap with lenses (middle), and housing (bottom).

### 2.1.3. System Integration

While deciding how to integrate the fNIRS sensors into the AttentivU frame we considered signal quality as well as how comfortable and similar to a normal pair of glasses the final device would be. Changes in cognitive load can best be detected in the prefrontal cortex (PFC) [1]. Siddiquee et al. [2020] found that the middle of the forehead is the optimal sensing location for monitoring cognitive load. The forehead is also the most common sensing location for wearable fNIRS devices because thick, dark hair blocks some of the infrared light and reduces the signal quality [Khan et al., 2012]. However, we eliminated the option of a forehead sensor as it would draw significant attention from others and reduce user acceptance. In order to minimize attenuation caused by hair in certain users we decided to mount Blueberry sensors on the temples of the AttentivU glasses above the lateral PFC where there is no hair.

Although fNIRS is less sensitive to motion artifacts than EEG, optode slippage may still produce spike-like artifacts. To improve the stability of our design we decided to mount a Blueberry sensor on each side of the AttentivU glasses frame using flat tension springs as shown in *Figure 5*. The springs lightly push the optodes into the user's head while allowing slight rotation about the vertical axis to accommodate various head shapes and sizes while reducing motion artifacts and minimizing light leakage by maintaining good scalp contact. The springs are slotted into 3D printed clips that wrap around the AttentivU glasses of which there are two sizes to accommodate an even wider range of head sizes.

To be able to compare the signal quality from the lateral PFC with the typical sensing location in the middle of the forehead during the study, we placed an extra Blueberry device on each

subject's forehead using a headband. We chose a thin, light-colored headband and performed preliminary tests to ensure that the fabric did not interfere with the lateral Blueberry sensors mounted on the glasses.

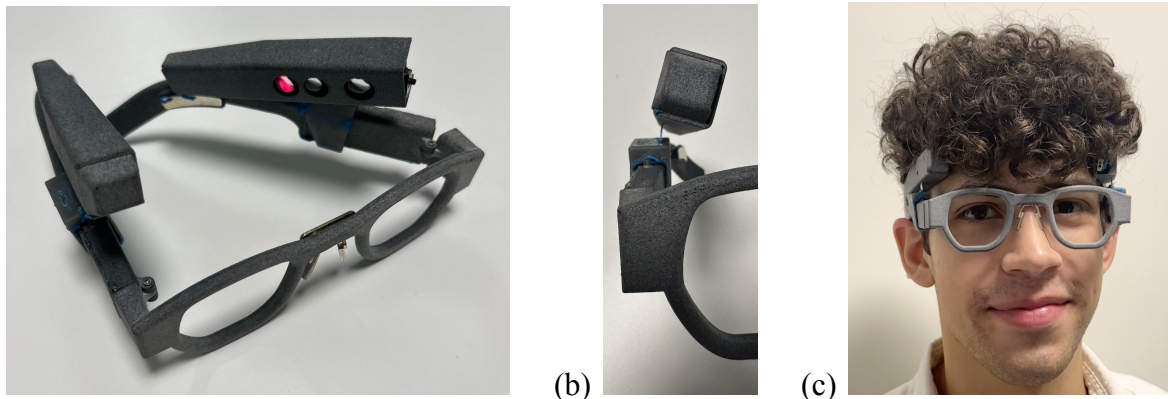


**Figure 5:** (a) Integrated EEG-fNIRS glasses consisting of two Blueberry fNIRS sensors and the AttentivU EEG/EOG glasses, (b) Blueberry device mounted on AttentivU glasses, (e) Image of a person wearing device

## 2.2. Participants

14 university students (7 women,  $22.5 \pm 2.2$  years old) with normal or corrected to normal vision and no history of neurological disorders were recruited to participate in this study. The study was approved by the ethics committee of MIT and the subjects were compensated for their time with a gift card.

## 2.3. Experimental Protocol

We chose to modulate cognitive load using mental arithmetic (MA) tasks. MA involves key cognitive processes including attention, working memory, decision making, and fact retrieval [Menon et al. 2010]. Hwang et al. [2014] conducted a comparative analysis of MA and n-back tasks which are the most common experimental paradigms used to induce cognitive load. They determined that MA was more consistent and robust with less training time and task adaption. MA may be initiated by different stimulus modalities (i.e. auditory or visual) or may be performed completely internally (i.e. imagined problems).

Subjects completed our experiment, which is outlined in *Figure 2.4*, while seated at a computer in a quiet room. The experiment took about 90 minutes and had six parts which all began with instructions. The first three parts had ‘regular timing’ and lasted 9 minutes and 30 seconds. They consisted of 10 sets of alternating MA and rest periods which were each 28 seconds long.

The next three parts had ‘random timing’ and lasted 14 minutes and 10 seconds each. They also included 10 sets of alternating MA and rest. The MA periods were exactly the same as in the first three parts but the rest duration was randomly chosen so the subject couldn’t predict when the next MA would start. During data analysis, 10 rest periods lasting 28 seconds each were randomly selected from each random rest period.

Each of the three regular timing and random timing parts used different stimuli for mental arithmetic. The three stimulus types, whose order was randomly chosen for each subject, were visual, auditory, and imagined. During MA periods with visual stimuli, an addition problem was displayed every 4 seconds (7 problems in total). During MA periods with auditory stimuli, an addition problem was read out loud using a Python text-to-speech module every 7 seconds (4 problems in total). The two operands for each addition problem were randomly generated 2-digit numbers. Subjects were instructed to do their best to solve each problem in their head and move on to the next problem once it was presented even if they didn't finish the last problem. During the MA periods with imagined stimuli, subjects were instructed to come up with addition problems themselves before solving them.

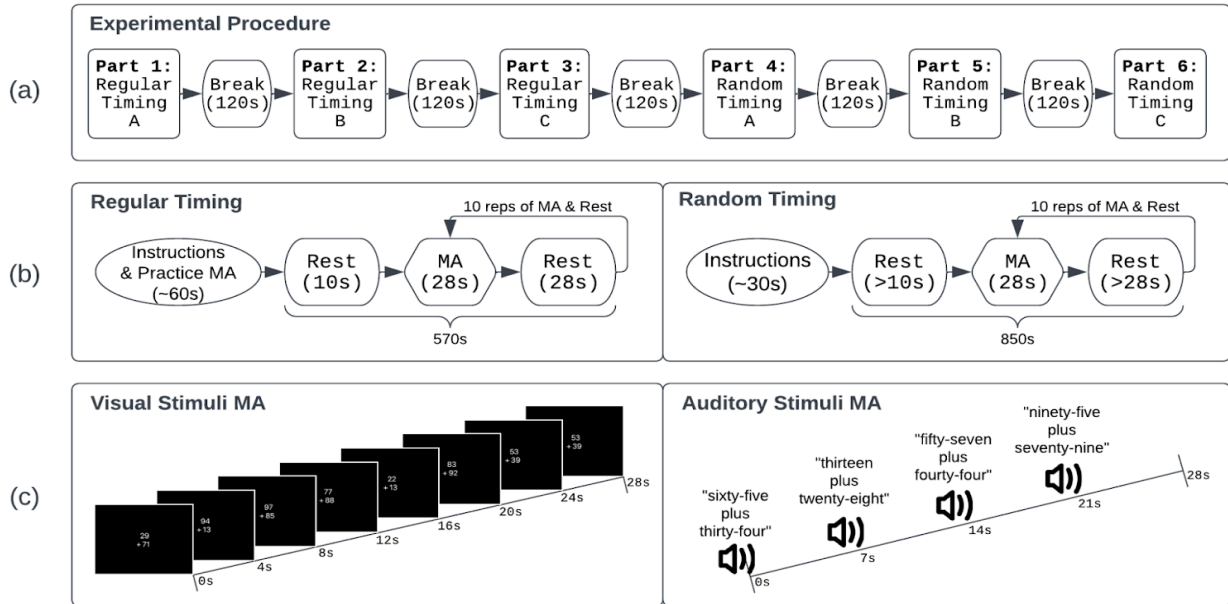


**Figure 6:** (a) Experimental procedure, (b) timing types, and (c) stimuli types

## 2.4. Preprocessing

Python was used for the preprocessing and analysis of the EEG and fNIRS data as described below.

The EEG data was first notch filtered at 60 Hz with a bandwidth of 10 Hz to remove line noise. Then, a Kaiser window finite impulse response bandpass filter with a passband of 1-60 Hz was applied. Finally, we performed Z-score normalization.

The fNIRS data was segmented into each of the six experiment parts. Then, the light intensity ( $I$ ) measurements for each optode and wavelength ( $\lambda$ ) were converted to changes in optical density ( $\Delta OD$ ) using the following equation.

$$\Delta OD(\lambda, t) = -\ln \left( \frac{I(\lambda, t)}{I_{avg}(\lambda)} \right)$$

Next, short-channel regression was performed to isolate the cerebral component of the optical densities ( $\Delta OD_{cerebral}$ ) using the equation given by Fabbri et al. [2004].  $Long$  denotes the optode

with 27 mm SDS while *short* denotes the optode with 10 mm SDS. The parameter  $\alpha$  was calculated using the least-squares approach described by Saager and Berger [2005].

$$\Delta OD_{cerebral}(\lambda, t) = \Delta OD_{long}(\lambda, t) - \alpha \cdot \Delta OD_{short}(\lambda, t)$$

$$\alpha = \frac{\Delta OD_{long}(\lambda, t) \circ \Delta OD_{short}(\lambda, t)}{\Delta OD_{short}(\lambda, t) \circ \Delta OD_{short}(\lambda, t)}$$

The corrected optical densities were used to calculate the concentration changes of HbO and HbR according to the MBLL [Delpy et al. 1988]. In our case, the SDS d was 2.7 cm and was scaled by the unitless differential pathlength factor (DPF) at each wavelength to estimate the average distance light traveled through the head. The DPFs were calculated using the equation derived from measurements of the frontal head by Scholkmann and Wolf [2013]. We used the specific molar absorption coefficients of HbO and HbR ( $\text{cm}^{-1}\text{mM}^{-1}$ ) measured by Matcher et al. [1995] for our wavelengths (740, 850, and 940 nm respectively).

$$\begin{bmatrix} \Delta[HbO](t) \\ \Delta[HbR](t) \end{bmatrix} = (A^T A)^{-1} A^T \begin{bmatrix} \Delta OD(\lambda_1, t) \div (d \cdot DPF(\lambda_1, age)) \\ \Delta OD(\lambda_2, t) \div (d \cdot DPF(\lambda_2, age)) \\ \Delta OD(\lambda_3, t) \div (d \cdot DPF(\lambda_3, age)) \end{bmatrix}$$

$$A = \begin{bmatrix} \alpha_{HbO}(\lambda_1) & \alpha_{HbR}(\lambda_1) \\ \alpha_{HbO}(\lambda_2) & \alpha_{HbR}(\lambda_2) \\ \alpha_{HbO}(\lambda_3) & \alpha_{HbR}(\lambda_3) \end{bmatrix} = \begin{bmatrix} 0.4920 & 1.3411 \\ 1.1596 & 0.7861 \\ 1.3520 & 0.7874 \end{bmatrix}$$

$$DPF(\lambda, age) = 223.3 + 0.05624 \cdot age^{0.8493} - 5.723 \cdot 10^{-7} \cdot \lambda^3 + 0.001245 \cdot \lambda^2 - 0.9025 \cdot \lambda$$

After the hemoglobin concentration changes were found for each fNIRS device, the results were filtered using a third-order Butterworth zero-phase band-pass filter with a passband of 0.01–0.1 Hz to remove any remaining noise.

## 2.5. Classification

Our main objective was to examine the potential benefits of fusing low-channel EEG and fNIRS in practical consumer BCIs. To validate this approach, offline binary classification between MA and rest periods for each subject and part of the experiment was performed for EEG and NIRS separately but also in combination using a meta-classifier.

The preprocessed EEG data was segmented using a sliding window with a 2 second duration and 1 second stride. An SVM and a CNN were trained for each subject and experiment part using 65, 20, and 15% of the data for training, validation, and testing respectively.

The fNIRS data was divided into epochs from -8 to 28 seconds where 0 is the start of a MA or rest period. Feature vectors were constructed using a sliding time window with a 4 second duration and a 2 second step size. The selected features included mean, max, min, std, kurtosis, skew, and slope of each window for HbO and HbR [1]. An SVM with a linear kernel was used for classification.

Buccino et al. [2016] showed that the highest accuracy is reached when EEG and fNIRS features are used together to train a classifier. Thus we concatenated the fNIRS and EEG feature vectors to train an SVM as a joint classifier. To prevent overfitting, five-fold cross-validation was used for each classifier.

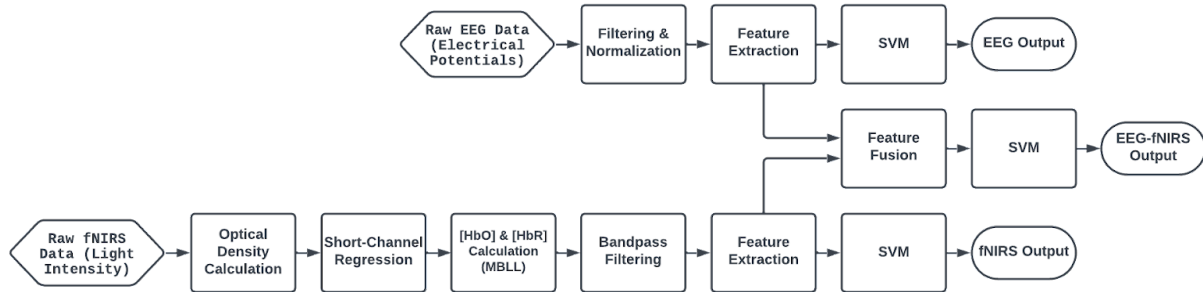


**Figure 7:** Flow diagram of data preprocessing and analysis pipeline

### 3. Results

The overall average classification accuracy only using the two EEG channels and one EOG channel was 69.6%. The

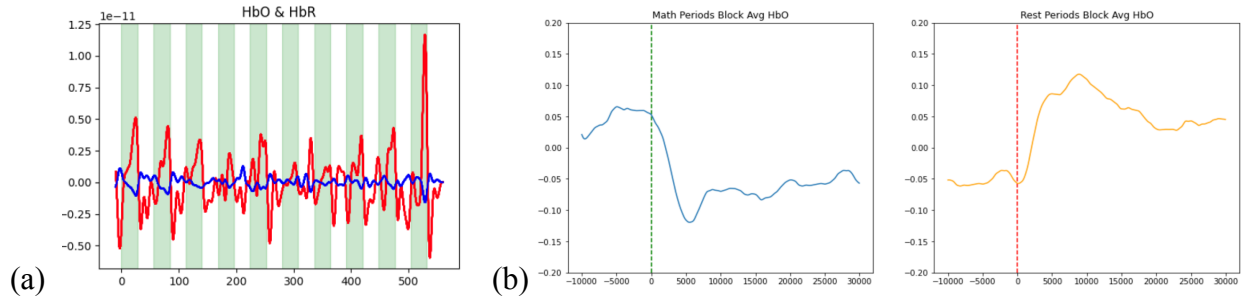


**Figure 8:** (a) Example of preprocessed HbO (red) and HbR (blue) data during alternating rest (green) and MA (white) periods (b) Block average of preprocessed HbO data for math and rest periods.

The classification accuracies for EEG, fNIRS, and EEG-fNIRS combinations for MA tasks are shown in Table 3. Compared with the averaged accuracy of the single mode EEG, there was an average \_% increase in classification accuracy for the bimodal EEG-fNIRS. Compared with the average accuracy of the single mode fNIRS, there was an average \_% increase in classification accuracy for the bimodal EEG-fNIRS system.

To compare the classification effect among single mode EEG, single mode fNIRS, and bimodal EEG-fNIRS, we used one-way repeated measures ANOVA to test the difference between the averaged classification accuracies based on the three kinds of signals. We found that the main effect in the ANOVA was significant ( $F = \text{_,}_p < 0.001$ ), meaning that there was a statistically significant difference between the three signals. Thus, post hoc tests were used to provide detailed information on which classification accuracies were significantly different from the others. Our results indicated that the averaged accuracy of the bimodal EEG-fNIRS was

significantly higher than that for both the single mode EEG and fNIRS (EEG-fNIRS vs. EEG,  $p < 0.01$ ; EEG-fNIRS vs. fNIRS,  $p < 0.001$ ). Moreover, the average classification accuracy for the single mode fNIRS was significantly higher than that for the single mode EEG ( $p < 0.001$ ).

The single mode EEG showed the lowest classification accuracy, whereas the bimodal EEG-fNIRS was optimal for almost all participants. Our data suggest that there are large individual differences in classification accuracy of cognitive load given the low number of channels. Thus, a BCI system with one mode may be inappropriate for participants with extremely low accuracy, whereas use of the bimodal system can provide a higher classification accuracy.

SVM Classification Accuracies:

Timing	Stimulus	Subject										Mean	SD
		Zoey	Nader	David	Daniel	Khiem	Sam	Harry	Sven	Michelle			
Regular	Visual	77.7	45.1	51.3	70.8	48.7	68.6	63.4	50	62.8	59.8	11.4	
	Auditory	66.1	42.4	53.1	51.3	45.1	72.5	59.2	71.7	51.3	57.0	11.1	
	Mental	65.5	54.9	52.2	35.4	57.5	55.3	71.3	51.3	55.8	55.5	9.9	
Random	Visual	48.2	79.4	51.8	66.1	36.6	75.3	68.6	75.9	66.9	62.5	14.5	
	Auditory	47.3	75.9	54.4	45.5	62.5	64.5	55.6	50	36.6	54.7	11.7	
	Mental	48.2	62.5	28.6	48.2	55.3	67.3	64.9	62.5	61.6	55.6	12.2	
		58.8	60.0	48.6	52.9	51.0	67.25	63.8	60.2	55.8			

CNN Classification Accuracies:

Timing	Stimulus	Subject										Mean	SD
		Zoey	Nader	David	Daniel	Khiem	Sam	Harry	Sven	Michelle			
Regular	Visual	77.3	62.7	57.8	69.9	57.8	79.5	86.2	65	75.9	70.2	10.1	
	Auditory	67.8	61.5	61.5	61.5	56.6	69.8	79.1	65	55.4	64.2	7.3	
	Mental	53	74.7	55.4	56.6	57.8	81.9	68.7	55.4	62.7	62.9	10.1	
Random	Visual	96.4	96.4	48.8	85.7	60.7	75.3	57.8	83.3	85.7	76.7	17.2	
	Auditory	77.3	81	61.9	83.3	71.4	84.2	82.8	50	64.3	72.9	11.9	
	Mental	56	100	57.1	44.1	81	78.4	48.7	96.4	71.4	70.3	20.2	
		71.3	79.4	57.1	66.9	64.2	78.2	70.6	69.2	69.2			

**Figure 3.2:** EEG data classification accuracies of SVM (top) and CNN (bottom) by subject and experiment part.

**Figure 3.3:** SVM classification accuracy on fNIRS data from left, right, front, and both left+right Blueberry devices.

The classification accuracies for EEG, fNIRS, and EEG-fNIRS combinations for imagery tasks are shown in Table 1. Compared with the averaged accuracy of the single mode EEG, there was an average 6.5% increase in classification accuracy for the bimodal EEG-fNIRS. Compared with the average accuracy of the single mode fNIRS, there was an average 24.4% increase in classification accuracy for the bimodal EEG-fNIRS. To compare the classification effect among single mode EEG, single mode fNIRS, and bimodal EEG-fNIRS, we used one-way repeated measures ANOVA to test the difference between the averaged classification accuracies based on the three kinds of signals. We found that the main effect in the ANOVA was significant ( $F = 32.0, p < 0.001$ ), meaning that there was a statistically significant difference between the three signals. Thus, post hoc tests were used to provide detailed information on which classification accuracies were significantly different from the others. Our results indicated that the averaged accuracy of the

## 4. Discussion

We aimed to integrate fNIRS and EEG into BCI glasses that are practical and accurate enough for everyday use. Our classification results demonstrate that combining as few as three EEG channels and four fNIRS channels can help improve the accuracy of consumer-friendly BCIs. This finding is inline with previous research into multimodal BCIs that was done using research-grade devices with dozens of channels that are typically attached to the head using a cap and conducting gel. This ensures good contact with the scalp and broader data but. This makes them unsuitable for widespread adoption in the workplace or even at home despite their many potential applications. However, most consumer-grade BCIs are unimodal and have underwhelming accuracy compared to research-grade devices.

We hope that our findings serve as a first step towards developing consumer-grade Furthermore, low channel BCIs are typically not very robust to noise stemming from movements. fNIRS is not susceptible to electrophysiological noise stemming from

*We aimed to establish a lightweight hybrid BCI system by combining a portable NIRS with an economical EEG system. The classification results verified that the simultaneous use of EEG and NIRS data was beneficial to improve classification performance. In particular, all subjects (except one: VP001) showed increased performance when the hybrid modality was used (see Table 1). Some previous studies have already confirmed that a hybrid BCI system combining NIRS with EEG can improve system performance, but they used stationary and bulky devices, thereby limiting application outside the laboratory setting [32, 37]. Since our hybrid system was implemented by combining a portable NIRS with an economical EEG system, it can be widely used and easy to handle not only in laboratory settings but also in out-of-lab scenarios.*

*Even though we verified the feasibility of the hybrid neuroimaging system in a typical BCI scenario, it may also be used for neurorehabilitation purposes, such as restoring motor functions*

*lost in neurological disorders. In this study, MA was selected as a cognitive task to demonstrate the usability of our system because it is one of the stable and consistent cognitive tasks that can produce distinct task-relevant brain activation.*

## References

Meng J, Zhang S, Bekyo A, Olsoe J, Baxter B, He B. Noninvasive electroencephalogram based control of a robotic arm for reach and grasp tasks. *Sci Rep.* 2016;6(1):38565.

S. Brandl, J. Hohne, K.-R. Muller, and W. Samek, “Bringing BCI into everyday life: Motor imagery in a pseudo realistic environment,” in 2015 7th International IEEE/EMBS Conference on Neural Engineering (NER), 2015, pp. 224–227.

Patil AV, Safaie J, Moghaddam HA, Wallois F, Grebe R. Experimental investigation of NIRS spatial sensitivity. *Biomed Opt Express.* 2011 Jun 1;2(6):1478-93. doi: 10.1364/BOE.2.001478. Epub 2011 May 9. PMID: 21698012; PMCID: PMC3114217.

Muse: [https://www.researchgate.net/figure/Muse-Headband-Sensors\\_fig3\\_329909772](https://www.researchgate.net/figure/Muse-Headband-Sensors_fig3_329909772)

NeuroSky:

[https://www.researchgate.net/figure/NeuroSky-MindWave-headset\\_fig3\\_328834634/download](https://www.researchgate.net/figure/NeuroSky-MindWave-headset_fig3_328834634/download)